Structure and Distribution of Aggregates Formed after Heat-Induced Denaturation of Globular Proteins

Jean-Christophe Gimel, Dominique Durand, and Taco Nicolai*

Laboratoire de Physico Chimie Macromoléculaire, URA CNRS, Université du Maine, 72017 Le Mans Cedex, France

*Received July 19, 1993; Revised Manuscript Received November 1, 1993**

ABSTRACT: The structure of aggregates formed upon heat-induced denaturation of β-lactoglobulin at pH 7.0 and 0.1 M ammonium acetate is studied by dynamic and static light scattering and small-angle neutron scattering. The internal structure and size distribution of the aggregates is found to be independent of the heating conditions (70 and 76 °C) and concentration (0.4, 2.0, 10, 30 g/L). The aggregates are self-similar down to a length scale of about 5 nm with a fractal dimension $d_f = 2.02 \pm 0.02$. The experimental results are compatible with a power law aggregation number distribution with an exponential cutoff at a characteristic aggregation number s^*: $n(s) \propto s^{-\tau} \exp(-s/s^*)$. From explicit analysis of dynamic light-scattering results the polydispersity coefficient τ is found to be close to unity. The internal dynamics are intermediate between those of fully flexible polymers and rigid aggregates.

Introduction

The phenomenon of irreversible thermal aggregation of globular proteins in aqueous solutions has been known for a long time and is widely used in the food preparation and food processing industry. Nevertheless, the exact nature of this phenomenon is only partially understood. The heating of globular protein solutions provokes complex changes of the molecular conformation which lead the protein to exhibit hydrophobic areas on its surface.[1] The partially denatured proteins aggregate and eventually precipitate or form a gel depending on the concentration.[2,3] The aggregation rate increases strongly with increasing temperature and concentration. The kinetics of the aggregation and the aggregate structure depend on the intricate balance between attractive and repulsive forces between the particles. Ionic strength and pH play an important role in this process as they determine the net charge and the range of electrostatic interactions. For example, in the case of β-lactoglobulin at pH 2 and low ionic strength transparent gels can be obtained whereas at pH 7 and high ionic strength the gels are opalescent.[3]

This study is mainly focused on the characterization of soluble aggregates formed upon heating in solutions of β-lactoglobulin at pH 7 and 0.1 M ionic strength using various scattering techniques and size exclusion chromatography (SEC). In addition, the aggregation process can be used to study the applicability of various theoretical aggregation models proposed in literature.

Experimental Section

Sample Preparation. β-Lactoglobulin is a globular protein which in solution consists of a mixture of dimers and monomers. The monomeric molar mass is 1.8×10^4 g/mol, and the diameter is 3.6 nm.[3] The β-lactoglobulin used in this study is obtained from Sigma (ref L.0130, batch 98F8030) and is a mixture of the genetic variants A and B. The protein was dissolved in 0.1 M ammonium acetate to which 200 ppm of NaN_3 has been added to avoid bacterial growth. Ammonium acetate has been used because of its efficiency in minimizing secondary interactions with SEC columns. The pH was set at 7 by adding small quantities of 1 M NaOH. The samples were filtered through 0.1-μm pore size Anotop filters into glass vials that had been soaked in sulfochromide and rinsed with distilled water and ethanol.

The samples were heated in a thermostated bath at either 70.0 ± 0.2 or 76.0 ± 0.2 °C for different periods of time. Temperatures and heating times were chosen on the basis of a preliminary study of the kinetics of the aggregation process. A systematic investigation of the kinetics is currently being undertaken and will be published at a later stage. The aggregation is quenched by rapid cooling to room temperature. Light scattering experiments are performed on highly diluted samples so that effects of interaction and multiple scattering are suppressed. The samples remain stable at room temperature over a period of months without any detectable continuing aggregation or breakup of aggregates. Concentrations were determined by measuring the extinction at 278 nm using extinction coefficient 0.96 $g \cdot L^{-1} \cdot cm^{-1}$.

Experimental Methods. SEC experiments were performed at room temperature using a HAB Waters UHG and TSK PW5000 column in series and a differential refractive index detection system. The eluent is 0.1 M ammonium acetate.

Both SLS and DLS measurements have been performed on a MALVERN 4700 instrument in combination with an ion argon laser operating with vertically polarized light with wavelength λ = 488 nm or a helium neon laser operating at 633 nm, both from Spectra Physics. The range of scattering vectors covered is $3.0 \times 10^{-3} < q < 3.5 \times 10^{-2}$ nm^{-1} ($q = (4\pi n_s/\lambda) \sin \theta/2$, n_s and θ being the solvent refractive index and the angle of observation, respectively). The temperature is controlled by a thermostated bath and was set at 20 °C. Toluene has been used as a reference in the SLS measurements with a value of 4.0×10^{-5} cm^{-1} for the Rayleigh factor at 488 nm and 1.4×10^{-5} cm^{-1} at 633 nm.

DLS measurements have been performed in the so-called parallel mode which allows measurements of the correlation function over a wide time range on a logarithmic scale. In this mode relaxation times, τ_r, that differ by orders of magnitude can be probed in a single measurement. The measured intensity auto correlation functions are related to the field autocorrelation functions through the Siegert relation

$$G^2(t) = A(G^1(t))^2 + B \quad (1)$$

where A is a constant depending on the experimental setup. In many situations $G^1(t)$ can be written as a sum of exponential decays: $G^1(t) = \int A(\tau_r) \exp(-t/\tau_r) d\tau_r$. By numerically calculating the inverse Laplace transform, ILT, of $G(t)$ a distribution $A(\tau_r)$ of relaxation times is obtained which can be attributed to different relaxational processes of the system. However, the inverse Laplace transform is notoriously ill defined if the data contain noise. A number of computer routines are available which aim at producing a relaxation time spectrum without spurious peaks, but still containing all the relaxational modes of the system within a chosen time window. We have used REPES which in general gives results similar to the more commonly used CONTIN, but has a few calculational advantages and is quicker and easier in

* Abstract published in *Advance ACS Abstracts*, December 15, 1993.

0024-9297/94/2227-0583$04.50/0

use. For details on the application of DLS to the study of macromolecular solutions see, e.g., refs 5 and 6.

SANS experiments were performed at the Léon Brillouin Laboratory in Saclay on the PACE spectrometer. Measurements made at two different wavelengths (0.5 and 1.25 nm) were combined to give a larger scattering vector range: $6 \times 10^{-2} < q < 2$ nm^{-1}.

Results

Characterization of Native β-Lactoglobulin. The native protein was characterized using SEC, SLS, DLS, and SANS. The refractive index chromatogram of a mixture of β-lactoglobulin, ovalbumin, and myoglobin shows that the elution volume of β-lactoglobulin is much closer to that of ovalbumin with molar mass 4.3×10^4 g/mol than that of myoglobin with molar mass 1.69×10^4 g/mol. SLS yields an apparent weight average molar mass, $M_w = 3.0 \times 10^4$ g/mol at a concentration $C = 5$ g/L using the refractive index increment 0.193 mL/g at $\lambda = 488$ nm given by Perlman et al.[7] However, since both a displacement of the monomer–dimer equilibrium upon dilution toward monomers and weak repulsive interactions influence the concentration dependence of the scattered intensity, care has to be taken in the interpretation of light-scattering results. A more precise light-scattering study of native β-lactoglobulin is currently being undertaken and will be reported at a later stage. The correlation function obtained from DLS is well described by a single exponential decay with a q^2-dependent relaxation rate. The diffusion coefficient D was determined using $D = (\tau_r q^2)^{-1}$, and the Stokes radius, R_s, was calculated from the diffusion coefficient extrapolated to infinite dilution using the Stokes–Einstein relation

$$D_0 = \frac{kT}{6\pi\eta R_s} \tag{2}$$

where k is the Boltzmann factor and η the solvent viscosity. A value $R_s = 2.9 \pm 0.1$ nm was found. The q-dependence of neutron-scattering intensity measured at $C = 27$ g/L is consistent with that of two connected spheres with radius 1.7 nm and center to center distance 3.3 nm. All findings lead to the conclusion that β-lactoglobulin is mainly present as dimers at pH 7 and ionic strength 0.1 M in the concentration range studied, which is consistent with earlier findings in literature.[3,4]

Characterization of β-Lactoglobulin Aggregates. Aggregates formed after various heating times at 70 and 76 °C and at concentrations of 0.4, 2.0, 10, and 30 g/L were investigated using SEC, SLS, SANS, and DLS. Heating times are chosen such that the whole domain between the initial aggregation and the onset of gelation is covered.

Size-Exclusion Chromatography. Figure 1 shows typical chromatograms of aggregates formed after various heating times. Upon heating, a peak due to the formation of aggregates appears well separated from the peak due to the nonaggregated proteins. The aggregate peak increases both in width and in height with increasing heating time while the nonaggregated protein peak decreases. The average elution volume of the aggregates decreases implying an increasing average size. Since after a short heating time part of the aggregates are completely excluded, it is difficult to analyze quantitatively the aggregate distribution with the SEC columns used. The fraction of nonaggregated proteins, α, has been calculated from the area of the refractive index chromatogram and decreases almost exponentially as a function of heating time; see inset in Figure 1.

Static Structure Factor. The scattered light intensity of all samples was measured as a function of the scattering vector. The measured intensities need to be corrected for the contribution of residual nonaggregated proteins, and a reduced intensity is calculated:

$$I_r(q) = \frac{I(q) - \alpha I_0(q)}{(1-\alpha) I_0(q=0)} \tag{3}$$

Here $I_0(q)$ is the scattering intensity from the proteins before heating. In the limit of $q = 0$, $I_r(q)$ represents the weight average aggregation number, s_w, of the aggregates, i.e., the weight average molar mass of the aggregates normalized by the molar mass of the proteins before heating.

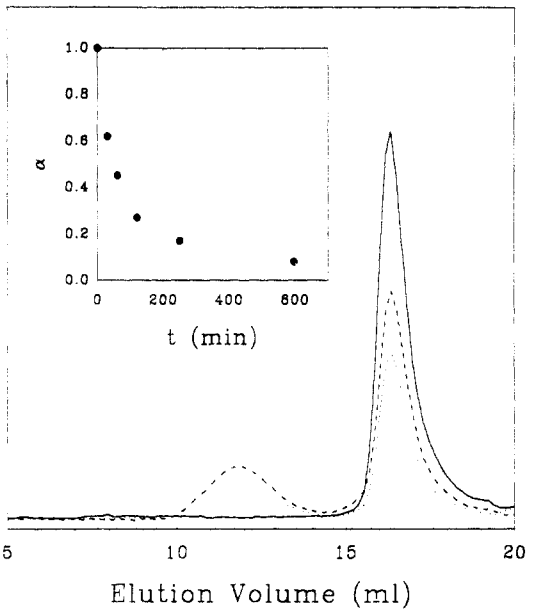

Figure 1. Refractive index signal as a function of the elution volume for aqueous solutions of β-lactoglobulin (pH 7; 0.1 M ammonium acetate; $C = 20$ g/L) before (solid) and after heating 30 min (dashed) and 60 min (dotted) at 76 °C. The native protein content as a function of heating time is shown in the inset.

In Figure 2 $I_r(q)$ is plotted as a function of the scattering vector for aggregates formed after various heating times at 76 °C at various concentrations. As was already apparent from the SEC measurements the average molar mass increases with increasing heating time. For the larger aggregates the internal structure can be probed within the q-range covered by light scattering. For very large aggregates the scattered light intensity has a power law dependence on the scattering vector over the whole accessible q-range and is independent of the overall size of the aggregates. In the case of self-similar aggregates $I \propto q^{-d_f}$ for $qR_g \gg 1$ where d_f is the apparent fractal dimension of the polydisperse aggregates. For β-lactoglobulin at pH 7 and ionic strength 0.1 M we obtain $d_f = 2.02 \pm 0.02$.

If the aggregates are self-similar independent of the heating time it should be possible to superpose the curves by normalizing the scattering vector with the z-average radius of gyration, $\langle R_g \rangle_z$, and $I_r(q)$ with s_w (we use $\langle R_g \rangle_z$ as a shorthand for $\langle R_g^2 \rangle_z^{0.5}$). The data shown in Figure 2a have been superposed in this way by choosing appropriate values of $\langle R_g \rangle_z$ and s_w, see Figure 2b. The near-perfect superposition implies that both the aggregates themselves and their distribution are self-similar over the accessible experimental range. Also plotted in Figure 2b are normalized data from aggregates formed at other concentrations and temperatures. There seems to be no difference in the internal structure of aggregates formed at the four concentrations and two temperatures investigated here while the aggregation rate varies by orders of magnitude.

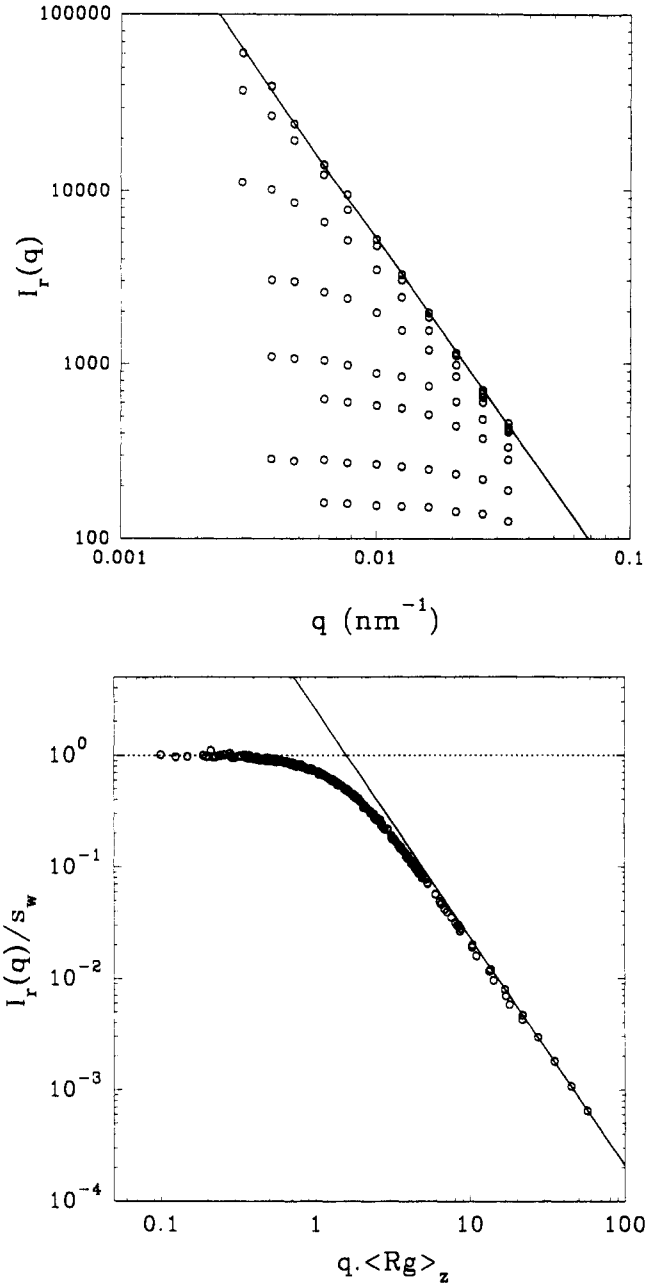

Figure 2. (a, Top) normalized scattered light intensities as a function of the scattering vector of aqueous solutions of β-lactoglobulin (pH 7; 0.1 M ammonium acetate) at various concentrations and heating times at 76 °C. The solid line has a slope −2.02 ± 0.02. (b, Bottom) the same data plus data obtained at other temperatures and concentrations are shown after normalization of the scattered light intensities by their value at $q = 0$ and the scattering vector by $\langle R_g \rangle_z$.

Values of s_w are plotted in Figure 3 as a function of the corresponding radius of gyration on a logarithmic scale. Within the experimental error a linear dependence is observed and a linear least-squares analysis gives

$$\langle R_g \rangle_z = 2.0 s_w^{0.505 \pm 0.005} \text{ nm} \quad (4)$$

This relationship provides an independent value of the fractal dimension since $\langle R_g \rangle_z \propto s_w^{1/d_f}$ where $d_f = 1.98$. The two values are consistent within the experimental error. The effect of polydispersity on d_f, which is the same for both the limiting slope of log I versus log q and the exponent in eq 4, will be discussed in the next section.

An extensive neutron-scattering study is currently being undertaken, the results of which will be published at a later stage. Here, we will show only results pertinent to the present study. Combined light- and neutron-scattering

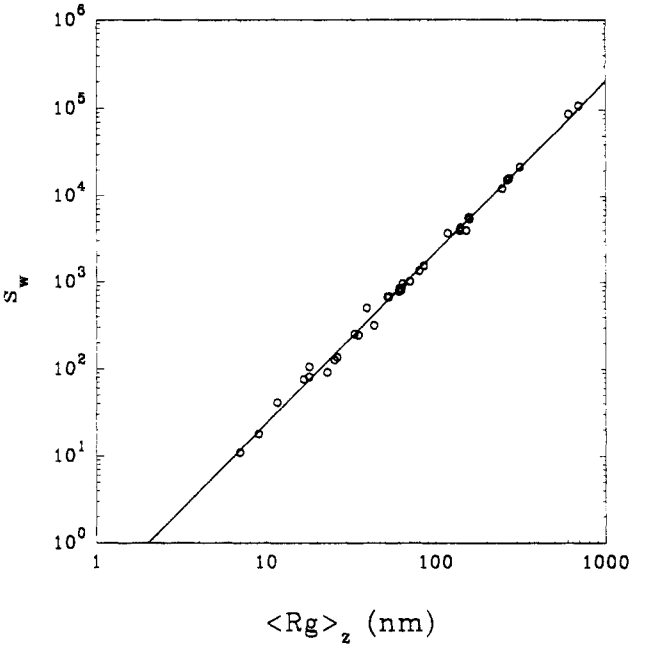

Figure 3. Weight average aggregation number as a function of the z-average radius of gyration. The solid line has a slope 1.98 ± 0.02.

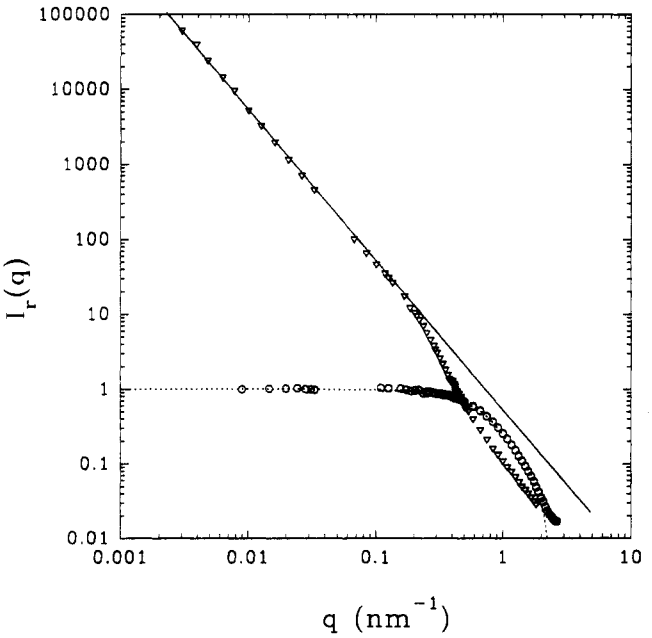

Figure 4. Combined SLS and SANS results for native β-lactoglobulin (pH 7; 0.1 M ammonium acetate) (○) and a solution containing very large aggregates showing the limiting behavior insensitive to further growth of the aggregates (▽). The dotted line represents the structure factor of two connected spheres (see text). The solid line has a slope of 2.0.

intensities for nonaggregated and highly aggregated β-lactoglobulin are shown in Figure 4 as a function of the scattering vector. The latter curve shows the limiting behavior over the whole q-range insensitive to further growth of the aggregates. The neutron-scattering intensities, which were not measured on an absolute scale, are adjusted to light-scattering data by a single shift factor. As mentioned above the static structure factor of native β-lactoglobulin is consistent with that of a dimer. The aggregates show a power law dependence over almost two decades until $q^{-1} \approx 5$ nm. At smaller distance scales the aggregates have a different, probably more compact, structure.

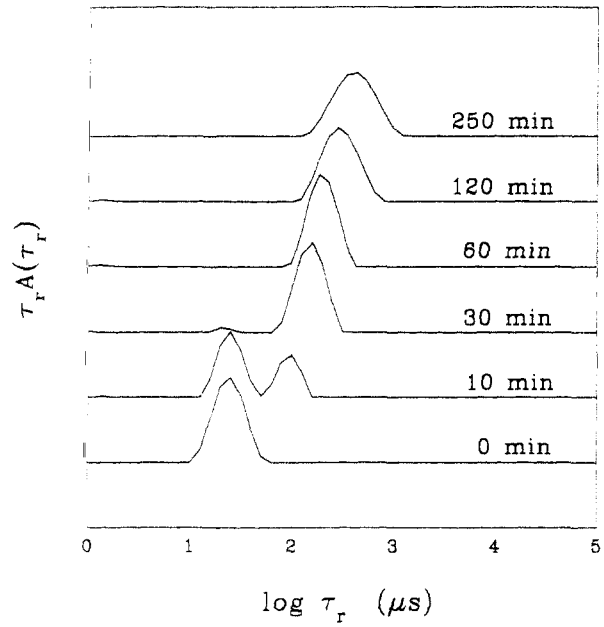

Figure 5. Relaxation time distributions obtained from an ILT of correlograms measured at $q = 1.17 \times 10^{-2}$ nm^{-1} for aqueous solutions of β-lactoglobulin (pH 7; 0.1 M ammonium acetate; C = 20 g/L) after various heating times. $A(\tau_r)$ has been multiplied by τ_r to give an equal area representation on a logarithmic scale.

Dynamic Light Scattering. DLS experiments were performed on most of the samples studied by SLS. Typical relaxation time distributions obtained from inverse Laplace transforms of the measured correlograms are shown after various heating times in Figure 5. In the early stage of the aggregation a fast relaxation time due to transitional diffusion of the not yet aggregated proteins can be observed separated from a peak at slower times due to translational diffusion of aggregates. The relaxation time spectrum, however, is quickly dominated by the aggregate peak which shifts to longer relaxation times with increasing heating time. For very dilute solutions only translational diffusion is expected to contribute to the relaxational process when $qR_g < 1$. If $qR_g > 1$ the relaxation time distributions broaden with increasing q due to contributions of rotation and internal modes, and the average relaxation time is no longer inversely proportional to q^2. The width of the relaxation time distribution can be characterized by comparing the harmonic average $\langle \tau_h \rangle$ with the arithmetic average $\langle \tau_a \rangle$.[8] These two averages are directly obtained from the measured correlation function using eq 1 and the following relations

$$\langle \tau_h \rangle = [\int_0^\infty \tau_r^{-1} A(\tau_r)\, d\tau]^{-1} = \left(-\frac{\partial \ln G^1(t)}{\partial t}\right)_{t\to 0} \quad (5)$$

$$\langle \tau_a \rangle = \int_0^\infty \tau_r A(\tau_r)\, d\tau = \int_0^\infty G^1(t)\, dt$$

where we have assumed that $\int_0^\infty A(\tau_r)\, d\tau = 1$.

The apparent diffusion coefficient has been calculated as $D_a = (\langle \tau_h \rangle q^2)^{-1}$ and is plotted in Figure 6a as a function of q for a number of different size aggregates. The z-average diffusion coefficient, $\langle D \rangle_z$, is the extrapolation of D_a at $q\langle R_g \rangle_z \ll 1$. For $qR_g > 1$ D_a increases with increasing q and shows again for the largest aggregate a power law dependence over the whole q range: $D_a \sim q^{-0.67\pm0.01}$. It is noted that although at a fixed q value the scattered light intensity is the same for all aggregates with $R_g > 10/q$, D_a continues to decrease. All the data can be superposed by normalizing q with $\langle R_g \rangle_z$ and D_a with $\langle D \rangle_z$; see Figure 6b.

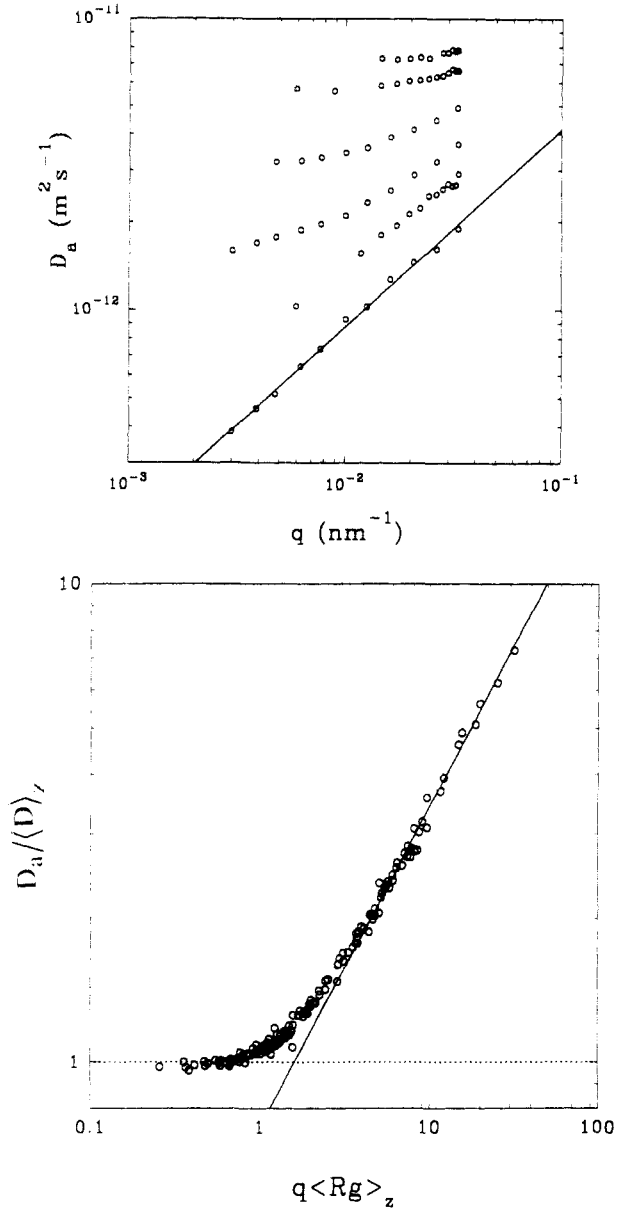

Figure 6. (a, Top) q-dependence of the apparent diffusion coefficient for aqueous solutions of β-lactoglobulin (pH 7; 0.1 M ammonium acetate) at different concentrations and heating times. The solid line has a slope 0.67 ± 0.01. (b, Bottom) the same data are plotted after normalization of D_a by the value at $q = 0$ and the scattering vector by $\langle R_g \rangle_z$.

The z-average Stokes radius, $\langle R_s \rangle_z$, calculated from $\langle D \rangle_z$, is close to the z-average radius of gyration obtained from the same sample. The ratio $\langle R_s \rangle_z / \langle R_g \rangle_z$ is plotted in Figure 7 as a function of s_w. The data show a rather large scatter mainly due to uncertainty in the determination of $\langle D \rangle_z$ with an average value 0.87 ± 0.05. Of course, for very small aggregates the ratio increases since for the native proteins it is 1.4.

The shape of the correlograms is a function only of $q\langle R_g \rangle_z$ as is illustrated in Figure 8 where $\langle \tau_a \rangle / \langle \tau_h \rangle$ is plotted as a function of $q\langle R_g \rangle_z$ for a number of samples with widely different values of $\langle R_g \rangle_z$. The scatter in the data is mainly due to the sensitivity of $\langle \tau_a \rangle$ to base-line noise.

Discussion and Conclusions

The results from static and dynamic light scattering imply that a power law distribution of self-similar aggregates is formed when solutions of β-lactoglobulin are heated at 70 or 76 °C. The kinetics of the aggregation process indicate a cluster–cluster-type aggregation.

The distribution function of the number of aggregates, $n(s)$, with aggregation number s can in most physically realistic types of cluster–cluster aggregation be written as[9]

$$n(s) \propto s^{-\tau} f(s/s^*) \tag{6}$$

where $f(s/s^*)$ is a cutoff function around a characteristic aggregation number s^*. Often an exponential cutoff function is used: $f(s/s^*) = \exp(-s/s^*)$. Two types of cluster–cluster aggregation have been studied intensively: reaction limited, RLCA, and diffusion limited, DLCA.[9] Fractal dimensions predicted by these models are 2.11 for RLCA and 1.75 for DLCA, while the polydispersity exponents, τ, are 0 and 1.5, respectively. The observed value of d_f excludes DLCA which is confirmed by the slow growth of the aggregates. The structure factor of the polydisperse system is related to that of the individual aggregates, $S_m(q)$, by

$$S(q) = \frac{\int_1^\infty s^2 n(s)\, S_m(q)\, ds}{\int_1^\infty s^2 n(s)\, ds} \tag{7}$$

Depending on the value of τ, the measured structure factor will be more or less influenced by polydispersity. Different combinations of $S_m(q)$ and τ can describe the experimental observations equally well, e.g., the structure factors of monodisperse Gaussian chains and of polydisperse computer-simulated RLCA aggregates[10] with $\tau = 1.2$ both give excellent fits to the data. However, the limiting slope is uninfluenced by polydispersity if $\tau < 2$.[11] Similarly, the exponent ν in the relations $\langle R_g\rangle_z = a_z \cdot s_w^{\nu}$ and $\langle R_s\rangle_z = b_z \cdot s_w^{\nu}$ is only influenced by polydispersity if $\tau > 2$. But the prefactors will be influenced even if $\tau < 2$. The ratios of the prefactors for monodisperse systems, a_m and b_m, to those for polydisperse systems are in our case, i.e., $\nu = 0.5$ (see eq 4):

$$\frac{a_m}{a_z} = \left[\left(\frac{\int_1^\infty s^2 n(s)\, ds}{\int_1^\infty s n(s)\, ds}\right)\left(\frac{\int_1^\infty s^2 n(s)\, ds}{\int_1^\infty s^3 n(s)\, ds}\right)\right]^{0.5} \tag{8}$$

$$\frac{b_m}{b_z} = \left(\frac{\int_1^\infty s^{1.5} n(s)\, ds}{\int_1^\infty s^2 n(s)\, ds}\right)\left(\frac{\int_1^\infty s^2 n(s)\, ds}{\int_1^\infty s n(s)\, ds}\right)^{0.5}$$

Thus, the influence of polydispersity on b_z is less important than on a_z. The ratio a_m/a_z varies between 0.816 and 0.396 for τ between 0 and 1.9, while b_m/b_z varies between 0.94 and 0.605.

Although we do not have a direct measure of τ, an approximate value can be obtained from SEC and DLS.

The SEC result can be related to the size distribution of the β-lactoglobulin aggregates using the calibration of the SEC column by pullulan standards and assuming that the Stokes radius of pullulan and β-lactoglobulin aggregates are the same if they have the same elution volume. This is an alternative of the more commonly used assumption of the so-called universal calibration where it is assumed that the intrinsic viscosities are the same for particles with the same elution volume. In fact, to calculate τ correctly the Stokes radii need only be proportional.[12] In this way a value $\tau = 1.0 \pm 0.2$ has been estimated. This value is obtained, however, only over the limited molar mass range not completely excluded by the column.

The ratio $\langle\tau_a\rangle/\langle\tau_h\rangle$ is a measure of the dynamic polydispersity, which is, however, directly related to the size distribution if $q\langle R_g\rangle_z \ll 1$. Assuming a size distribution given by eq 6 it is readily shown that for $\tau < 3 - 1/d_f$

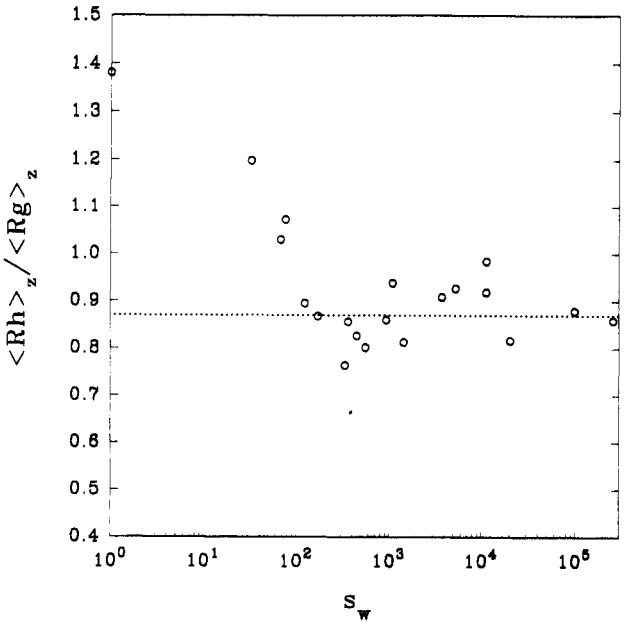

Figure 7. Ratio of the z-average Stokes radius to the z-average radius of gyration as a function of the weight average aggregation number.

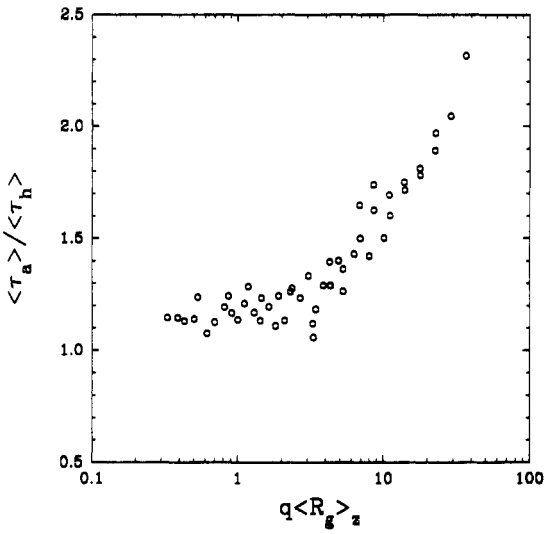

Figure 8. Ratio of the arithmetic to the harmonic average relaxation times versus $q\langle R_g\rangle_z$ for a number of samples with widely different values of $\langle R_g\rangle_z$.

$$\langle\tau_a\rangle/\langle\tau_h\rangle = \frac{\Gamma(3 + 1/d_f - \tau)\Gamma(3 - 1/d_f - \tau)}{\Gamma^2(3 - \tau)} \tag{9}$$

The experimentally observed value $\langle\tau_a\rangle/\langle\tau_h\rangle = 1.17 \pm 0.02$ leads to $\tau = 1.0 \pm 0.15$.

A third estimate of τ can be obtained by explicit analysis of the correlation functions. In dilute solutions at scattering angle such that $qR_g < 1$ for all aggregates, we can consider each aggregate as a point scatterer diffusing independently of other aggregates present. The relaxation time of each aggregate is related to its Stokes radius

$$\tau_r = R_s \frac{6\pi\eta}{kTq^2} \tag{10}$$

with $R_s = b_m \cdot s^{\nu}$. Taking $\langle R_s\rangle_z/\langle R_g\rangle_z = 0.87$ and neglecting the increase of $\langle R_s\rangle_z/\langle R_g\rangle_z$ for very small aggregates we obtain $R_s = 1.7(b_m/b_z)s^{0.5}$ nm if $\tau < 2$. The contribution of each particle to the relaxation time distribution is

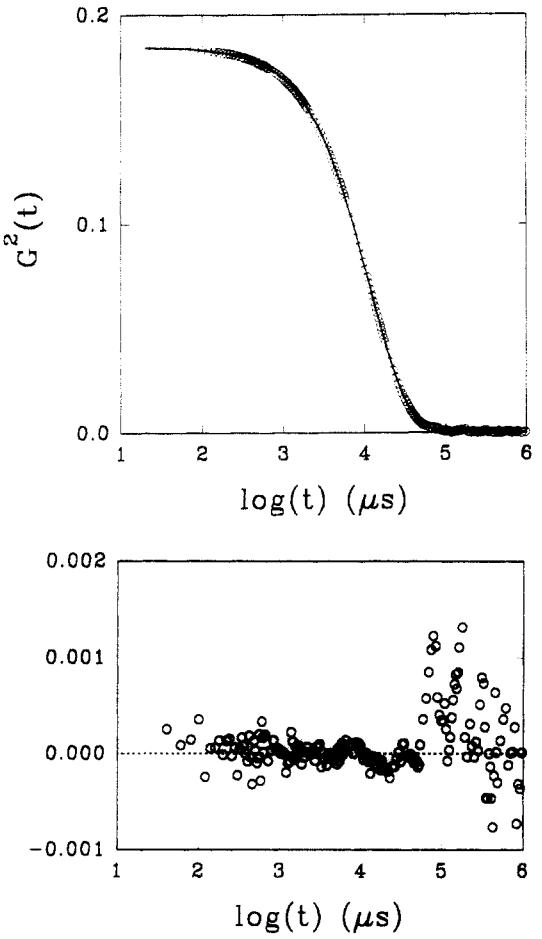

Figure 9. (Top) experimental correlation function measured at $q = 3.88 \times 10^{-3}$ nm^{-1} for aqueous solutions of β-lactoglobulin (pH 7; 0.1 M ammonium acetate; C = 10 g/L) after 30 min heating at 76 °C. The solid line is obtained from a nonlinear least-squares fit to eqs 1 and 12 where τ is a floating parameter. The residuals are shown in the bottom panel.

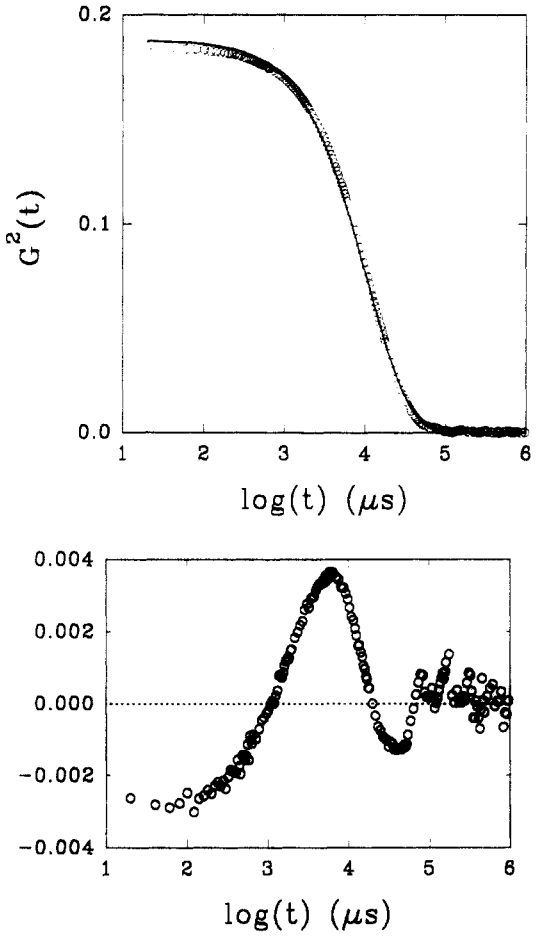

Figure 10. Same as Figure 9, but taking a fixed value $\tau = 2.0$.

proportional to its scattering intensity:

$$A(s) \propto s^2 \cdot n(s) \propto s^{2-\tau} \exp(-s/s^*) \tag{11}$$

The field autocorrelation function can therefore be written as

$$G^1(t) \propto \int s^{2-\tau} \exp(-s/s^*) \exp(-t/\tau_r)\, ds \tag{12}$$

with τ_r given by eq 10. The values for τ and s^* obtained from a fitting procedure can be used to calculate the weight average aggregation number which should be consistent with the value obtained from SLS:

$$s_w = \frac{\int_1^\infty s^{2-\tau} \exp(-s/s^*)\, ds}{\int_1^\infty s^{1-\tau} \exp(-s/s^*)\, ds} \tag{13}$$

The systems for which this type of analysis is suitable need to have a large enough average aggregation number so that the scattering from nonaggregated particles can be neglected, and eq 6 is a good representation of the mass distribution. On the other hand, the aggregates need to be small enough for the contribution of internal modes and rotation to be negligible at the lowest experimentally accessible scattering angle. Correlation functions measured on samples with $4000 > s_w > 300$ at scattering angles for which $q\langle R_g\rangle_z < 1$ could be superposed by a simple time shift and did not show a significant shape variation. This implies that in this range τ is constant. In Figure 9 a correlation function is shown measured at $q = 3.88 \times 10^{-3}$ nm^{-1} on a sample with s_w = 1010, $\langle R_g\rangle_z$ = 70.4 nm and $\langle R_s\rangle_z$ = 64.1 nm. The solid line through the data is the result of a fit to eq 1 with $G^1(t)$ given by eq 12. The residuals are shown in the bottom panel of Figure 9, and it is clear that the model describes the experimental data very well. The values obtained from the nonlinear least-squares analysis are τ = 1.1 and s^* = 1794. The value of s_w calculated using eq 13 is 1623. The difference with the value from SLS can be attributed to the uncertainty in the prefactor b_z; taking b_z = 2.1 nm results in an exact agreement. On the other hand τ is insensitive to the exact choice of b_z. Although the shape of the correlation function is not strongly modified by small variations in τ, we can exclude values widely different. This is illustrated in Figure 10 where the result of a fit with a fixed value τ = 2 is shown together with the residuals. The relaxation time distribution obtained from the fit with τ a floating parameter is compared in Figure 11 with simulated distributions with the same $\langle\tau_h\rangle$ and different values of τ.

All three estimates give a value for τ close to unity which means that the measured fractal dimension is not influenced by polydispersity. Using τ = 1 we obtain R_s/R_g = 1.05 ± 0.05 for monodisperse aggregates which is close to the value for RLCA aggregates.

The structure factor of the aggregates is probably close to that of RLCA aggregates since the $S(q)$ is well described by eq 7 using the structure factor of computer simulated RLCA aggregates and τ = 1.2.

It is well known that in order to form a gel the polydispersity of the system diverges and thus τ should be greater than 2. Since the system we are studying does in some cases eventually gel, one has to invoke a transition to a different aggregation process before the gel point. Since in this study no signs of such a transition have been

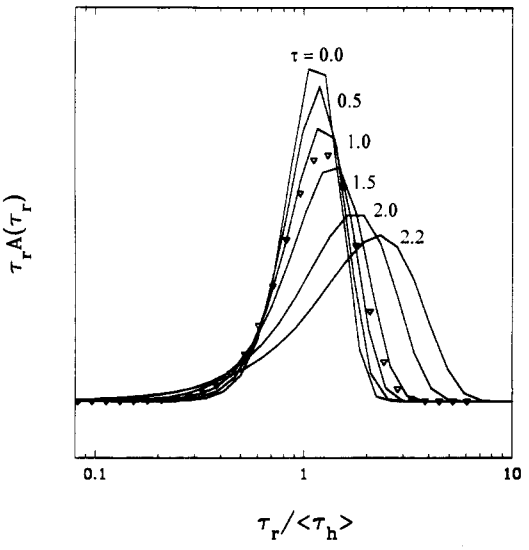

Figure 11. Comparison of relaxation time distributions with the same $\langle\tau_h\rangle$ for different values of τ. ▽ represent the result from a fit with τ as a floating parameter.

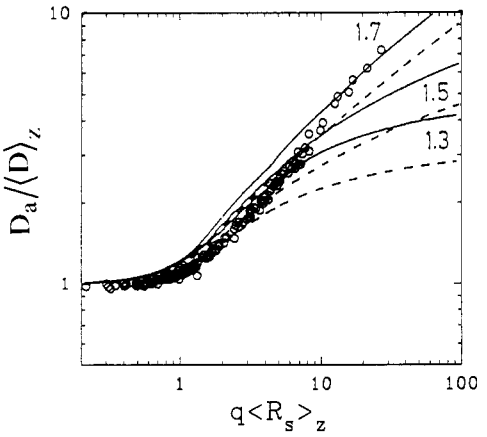

Figure 12. Comparison of the experimental ratio $D_a/\langle D\rangle_z$ (○) with values calculated by Klein et al.[10] for RLCA aggregates for different values of τ, with (—) and without (- -) the effects of rotational diffusion.

observed, it probably takes place very close to the gelation threshold.

Klein et al.[10] have calculated the effect of polydispersity and rotation on D_a for RLCA aggregates as a function of $q\langle R_s\rangle_z$. It is clear from Figure 12, where the experimental data are compared to these calculations, that rotation and polydispersity by themselves cannot fully explain the increase of D_a with increasing $q\langle R_s\rangle_z$. One needs to invoke some flexibility to explain the stronger increase. Since for flexible coils D_a increases linearly with $q\langle R_g\rangle_z$ for $q\langle R_g\rangle_z > 4$ the internal dynamics of β-lactoglobulin aggregates are intermediate between those of flexible coils and rigid aggregates. On the basis of the present data it is difficult to decide whether the internal dynamics have a different q-dependence and are therefore different in kind compared to flexible coils or whether the asymptotic regime is simply not yet reached. The continuous increase of the dynamic polydispersity suggests the latter option.

In conclusion, the structure of aggregates formed upon heat-induced denaturation of β-lactoglobulin at pH 7 and 0.1 M ionic strength is independent of the heating temperature and the concentration in the range covered by this study. The aggregates have a fractal dimension $d_f = 2.0$ down to a length scale of about 5 nm. The size distribution is well described by a power law dependence on the aggregation number with τ close to 1 and an exponential cutoff around a characteristic size. The apparent diffusion coefficient shows a power law dependence on q for $qR_g \gg 1$, which is, however, weaker than for fully flexible polymers.

Acknowledgment. We thank F. Boué and J. P. Busnel for their assistance with the SANS and SEC experiments, respectively.

References and Notes

(1) Cantor, C. R.; Schimmel, P. R. *Biophysical Chemistry*; Freeman and Company: San Francisco, 1980.
(2) Clark, A. H.; Lee-Tuffnell, C. D. In *Functional Properties of Food Macromolecules*; Mitchell, J. R., Ledward, D. A., Eds.; Elsevier Applied Science Publishers: London, 1986.
(3) Kinsella, J. E.; Whitehead, D. M. *Adv. Food Nutr. Res.* **1989**, *31*, 343.
(4) McKenzie, H. A. In *Milk Proteins: Chemistry and Molecular Biology*; McKenzie, H. A., Ed.; Academic Press: New York, 1971; Vol. 2.
(5) Brown, W., Ed. *Dynamic Light Scattering: The Method and Some Applications*; Clarendon Press: Oxford, 1993.
(6) Berne, B. J.; Pecora, R. *Dynamic Light Scattering*; Wiley & Sons: New York, 1976.
(7) Perlmann, E.; Longsworth, L. G. *J. Am. Chem. Soc.* **1948**, *70*, 2719.
(8) Martin, J. E. *Phys. Rev. A* **1987**, *36*, 3415.
(9) Vicsek, T. *Fractal growth phenomena*; World Scientific: London, 1989.
(10) Klein, R.; Weitz, D. A.; Lin, M. Y.; Lindsay, H. M.; Ball, R. C.; Meakin, P. *Progr. Colloid. Pol. Sci.* **1990**, *81*, 161.
(11) Martin, J. E. *J. Appl. Cryst.* **1986**, *19*, 25.
(12) Schosseler, F.; Benoit, H.; Grubisic-Gallot, Z.; Strazielle, Cl.; Leibler, L. *Macromolecules* **1989**, *22*, 399.